Size dependent carrier recombination in ZnO nanocrystals

G. Pozina,[1,a)] L. L. Yang,[2] Q. X. Zhao,[2] L. Hultman,[1] and P. G. Lagoudakis[3]
[1]*Department of Physics, Chemistry and Biology (IFM), Linköping University, SE-581 83 Linköping, Sweden*
[2]*Department of Science and Technology, Linköping University, Campus Norrköping, SE-601 74 Norrköping, Sweden*
[3]*School of Physics and Astronomy, University of Southampton, Southampton SO17 1BJ, United Kingdom*

(Received 17 August 2010; accepted 9 September 2010; published online 29 September 2010)

Experimental and theoretical studies of fluorescence decay were performed for colloidal ZnO nanocrystals. The fluorescence lifetime reduces from 22 ps to ~6 ps with decreasing nanocrystal radius. We postulate that non-radiative surface states dominate the carrier dynamics in small ZnO nanocrystals and perform Monte Carlo simulations incorporating carrier diffusion and carrier recombination to model the experimental fluorescence decay dynamics. The percentage of excitons undergoing nonradiative decay due to surface trapping is as high as 84% for nanocrystals with 8 nm radius, which explains the ultrafast decay dynamics observed in small ZnO nanostructures even at low temperatures. © *2010 American Institute of Physics*. [doi:10.1063/1.3494535]

ZnO is one of the most attractive wide-band gap semiconductors for optoelectronic applications due to its huge exciton binding energy of 60 meV, which allows to design devices operating at temperatures exceeding 300 K. Reduction in physical size to nanoscale offers interesting applications for nanophotonics and nanovoltaics. Low-cost ZnO nanostructures have strong potential for fabrication of light-emitting diodes, nanolasers, nanosized sensors of high sensitivity and field emitters.[1–3] Since nanocrystals (NCs) possess a relatively large surface with respect to their volume the influence of surface recombination might be significant for some important applications such as light emitters or solar-cells based on ZnO NCs. From this point of view it is necessary to understand in quantitative terms how the NC size affects the fluorescence properties of ZnO. In this paper, we report results of time-resolved fluorescence studies and model the dynamics using Monte Carlo simulations.

ZnO NCs are synthesized at 200 °C by a chemical precipitation method from the water solution of $ZnCl_2$ (1:2) dropped slowly in the solution of NH_4HCO_3 mixed with dodecyl sodium sulfate (for details see Ref. 4). The geometrical parameters of the nanocrystals are confirmed by transmission electron microscopy (TEM) measurements using an FEI Technai G2 200 keV FEG instrument. While TEM analysis shows that even though the ZnO nanocrystals reveal a slightly hexagonal shape, it is meaningful to approximate them as spherical bodies with an average radius of 8 nm for the as-grown NC [see Figs. 1(a) and 1(b)]. The bigger NCs are obtained by heating in different atmospheres and temperatures. Annealing during 1 h at 300 °C in air results in increase of the average grain radius to R =15 nm [Fig. 1(c)]. The average radius is estimated to 30 nm and 35 nm after annealing at 500 °C in forming gas [mixture of Ar and O_2 (1:1)] and in air, respectively, [Figs. 1(d) and 1(e)]. The grain radius of 45 nm is obtained after heating at 700 °C in air [Fig. 1(f)]. We photoexcite the NCs nonresonantly using the third harmonics (λ_e=266 nm) from a Ti:sapphire 180 fs mode-locked laser with a repetition frequency of 75 MHz.

Figure 2(a) shows normalized fluorescence spectra (solid lines) and absorption spectra (dashed red lines) measured at T=300 K for NCs with the average radius R of 8, 15, and 45 nm. The room temperature fluorescence and the absorption maxima for five different NC diameters are shown in Fig. 2(b) suggesting of exciton quantum confinement for NCs with radii up to 35 nm. We also observe an increasing Stock shift between the fluorescence and absorption maxima with decreasing NC size, reaching ~120 meV for NCs of R=8 nm. The Stock shift size dependence was previously attributed to the additional confinement from surface traps.[5] Figure 2(c) shows the fluorescence spectrum of the 45 nm ZnO NCs at different temperatures. At 5 K we observe that

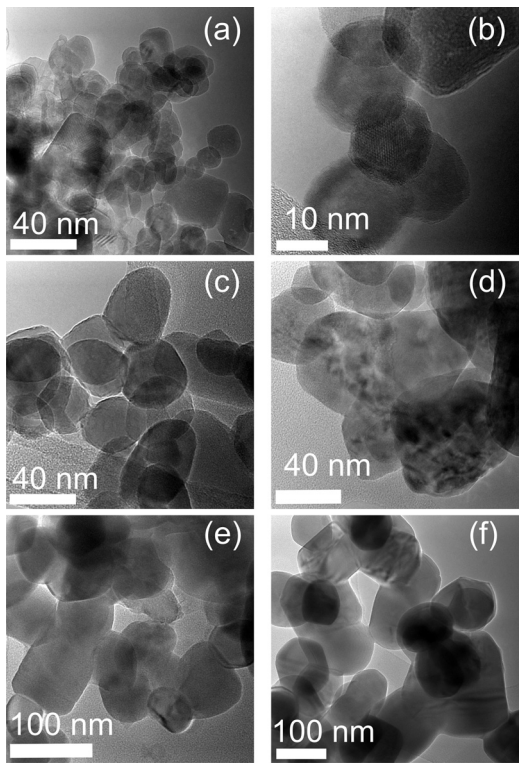

FIG. 1. TEM images are shown for ZnO NCs with an average radius of 8 nm [(a) and (b)], 15 nm (c), 30 nm (d), 35 nm (e), and 45 nm (f). Image on (b) illustrates that nanoparticles have single crystal quality.

[a)]Electronic mail: galia@ifm.liu.se.

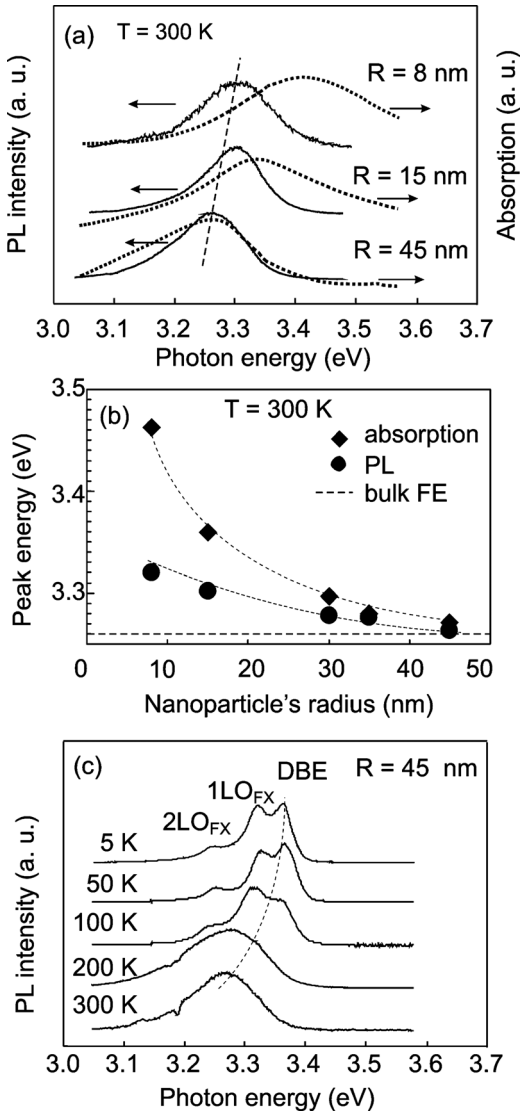

FIG. 2. (a) Normalized fluorescence spectra measured at 300 K and the corresponding room-temperature absorption spectra (dashed lines) for NCs of different radius. (b) The fluorescence (solid circles) and absorption (solid rhombs) peak energy as a function of NCs radius. The thin dashed lines are guide for the eye. (c) Normalized fluorescence spectra measured at different temperatures for NCs with an average radius of 45 nm.

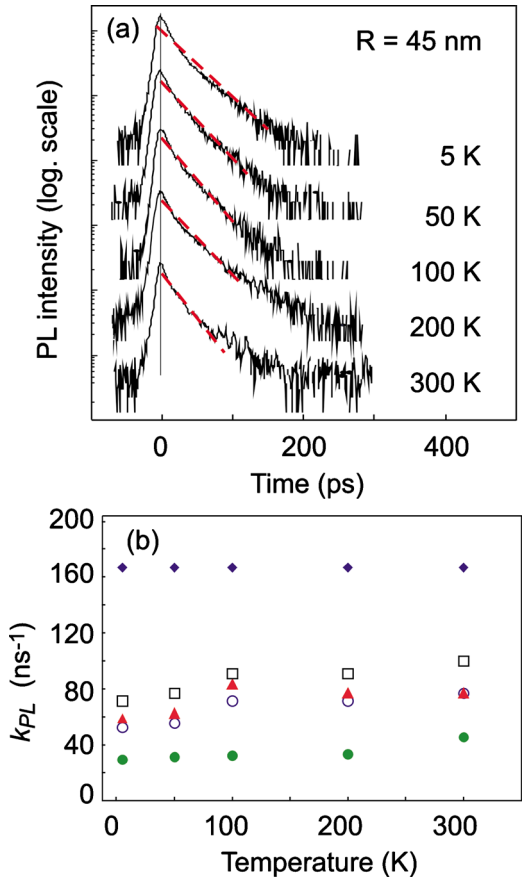

FIG. 3. (Color online) (a) Fluorescence decay curves taken at different temperatures for NCs with R=45 nm. The fit using a single exponential law is shown by dashed lines. (b) Extracted decay rate is shown for NCs of different size: by solid rhombs for R=8 nm, by open squares for R =15 nm, by solid triangles for R=30 nm, by open circles for R=35 nm, and by solid circles for R=45 nm, respectively.

the spectrum is rather similar to bulk ZnO fluorescence with a dominating donor bound exciton (DBE) peak at ~3.36 eV and the first and second LO-phonon replicas of the free exciton at ~3.32 eV and 3.25 eV, respectively.[6] The fluorescence spectra measured at higher temperatures demonstrate a broad emission band related to the free exciton transitions as bound excitons are expectedly quenched.

Characterization of the competition between exciton trapping at donor impurities and nonradiative exciton recombination for NCs of different sizes allows us to deduce the nature of the nonradiative channels in ZnO NCs. Figure 3(a) shows the fluorescence decay of 45 nm NCs for different temperatures. We observe a fastening of the fluorescence decay rate with increasing temperature, which is congruent with the thermal activation of nonradiative channels and the shorter lifetime of free excitons compared to donor bound excitons. We approximate the fluorescence decay rate by fitting an exponential to the fluorescence decay curves. Figure 3(b) shows the fluorescence decay rates as a function of temperature for different NCs sizes. We observe that for small NCs the fluorescence decay rate remains virtually unaffected suggesting that in small nanocrystals nonradiative recombination of free excitons dominates over the formation of donor bound excitons. Such temporal behavior of fluorescence for small NCs is different when compared to epitaxial or bulk ZnO, where lifetimes for both free and bound excitons change (decrease) with increasing temperature. In colloidal NCs as the surface to volume aspect ratio increases with decreasing size the annihilation occurs predominantly at nonradiative surface states.

We use Monte Carlo for a quantitative analysis of carrier dynamics in ZnO NCs. The studied ZnO nanocrystals are considered as ideal spherical bodies of radius R. In the model, we assume that the initial population of excitons created under a short laser pulse in a sphere of radius R is N and excitons are distributed randomly within the spherical body. Excitons are assumed free particles at 300 K when all shallow traps are ionized. Furthermore, since R is larger than the exciton Bohr radius we can treat the exciton movement as a three-dimensional motion of a point particle having thermal velocity with the magnitude of 122 nm/ps obtained from

$$v = \sqrt{3k_B T/m_{ex}},$$

where m_{ex} is an exciton mass in ZnO, calculated using the electron and the hole effective masses of $0.25m_0$ and $0.66m_0$ for the upper valence band, respectively.[7] Excitons diffuse in a random trajectory within the sphere due to collisions with

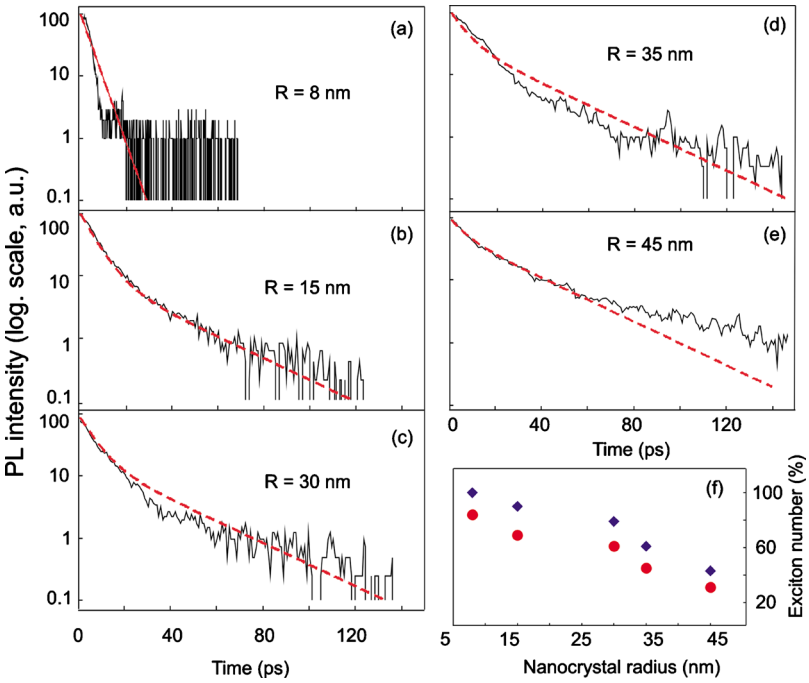

FIG. 4. (Color online) Room temperature normalized fluorescence decays (solid lines) for NCs of different size with radii (a) 8 nm, (b) 15 nm, (c) 30 nm, (d) 35 nm, and (e) 45 nm, together with the corresponding results using Monte Carlo (dashed lines). (f) Percentage of excitons, which decay nonradiatively inside the NCs (circles), and percentage of excitons, which decay in the "edge" area (rhombs) are shown as a function of NCs size.

impurities or phonons and the probability of scattering processes is described by the electron momentum scattering time of $\sim 10^{-3}$ ps.[8] We assume that excitons can undergo radiative or nonradiative annihilation depending on their position inside the NC. We consider two regions within the NC: (i) internal volume, where excitons recombine radiatively and (ii) "edge" area, in which excitons are getting bound to the surface states and can annihilate both radiatively and nonradiatively. The thickness of the "edge" spherical shell is taken to be 8 nm ($\sim 4a_B$, where $a_B \approx 2$ nm is the exciton Bohr radius[6]). The probability of radiative decay is given by $k_r = 1/25$ ps^{-1} corresponding to the bulk ZnO recombination rate measured at 300 K and the probability of nonradiative decay is described by the rate $k_{nr} = 1/8$ ps^{-1} for all NCs, but the 8 nm radius, where we used $k_{nr} = 1/5$ ps^{-1} optimized to fit the experimental fluorescence decay curves assuming a biexponential decay, as follows:

$$I(t) = \frac{N_i}{N}\exp(-k_r t) + \frac{N_s}{N}\exp[-(k_r + k_{nr})t],$$

where N_i/N and N_s/N are the calculated fraction of excitons annihilate inside the internal area and inside the "edge" region, respectively, using Monte Carlo simulation. Normalized experimental fluorescence decay curves (solid lines) together with Monte Carlo simulations (dashed lines) are shown in Fig. 4 for NCs of different size. All calculated curves are obtained using the same parameters except the NCs radius. Figure 4(f) shows the dependence of the percentage of excitons suffering nonradiative decay with the NCs size (circles). We found that ~43% of all excitons decay in the "edge" area and the percentage of excitons, which undergo nonradiative recombination is ~31% for the NC with the biggest radius of 45 nm. In the intermediate case, for the ZnO NC with $R = 15$ nm, the percentage of excitons undergoing nonradiative recombination is ~69%. For the smallest NC with $R = 8$ nm, more than ~84% of all excitons annihilate nonradiatively at the surface area. The percentage of excitons decaying at the surface area of the NCs versus NC size is shown by rhombs in Fig. 4(f). Monte Carlo simulation performed for 5 K gives only negligible change (~1%) to the percentage of all excitons undergoing nonradiative recombination, which is consistent with a very short fluorescence decay time measured for these NCs at low temperature. The above model neglects the enhancement of the light-matter coupling strength and the retardation (exciton-polariton) effect with increasing NC size since these phenomena are predicted to be less important for small ZnO quantum dots.[9]

In summary, we have observed that fluorescence lifetime reduces from 22 to ~6 ps with decreasing NC radius. The dominance of nonradiative surface recombination is confirmed by Monte Carlo simulations of the fluorescence decay. In NCs with $R = 8$ nm the calculated percentage of excitons recombining nonradiatively within the surface area exceeds 84%, which explains the unusually short fluorescence lifetime measured in such small ZnO NCs.

This work was supported by the Swedish Research Council (VR), the Swedish Energy Agency, The Swedish Governmental Agency for Innovation Systems (VINNOVA), EPSRC under Grant Nos. EP/F013876/1 and EP/G063494/1, and the FP7 Network of Excellence Nanophotonics for Energy Efficiency.

[1]Z. W. Pan, Z. R. Dai, and Z. L. Wang, Science **291**, 1947 (2001).
[2]Z. L. Wang, X. Y. Kong, Y. Ding, P. Gao, W. L. Hughes, R. Yang, and Y. Zhang, Adv. Funct. Mater. **14**, 943 (2004).
[3]Z. L. Wang, J. Phys.: Condens. Matter **16**, R829 (2004).
[4]J. H. Yang, X. Y. Liu, L. L. Yang, Y. X. Wang, Y. J. Zhang, J. H. Lang, M. Gao, and B. Feng, J. Alloys Compd. **477**, 632 (2009).
[5]S. Yamamoto, H. Yano, T. Mishina, and J. Nakahara, J. Lumin. **126**, 257 (2007).
[6]Ü. Özgür, Ya. I. Alivov, C. Liu, A. Teke, M. A. Reshchikov, S. Doğan, V. Avrutin, S.-J. Cho, and H. Morkoç, J. Appl. Phys. **98**, 041301 (2005).
[7]N. N. Syrbu, I. M. Tiginyanu, V. V. Zalamai, V. V. Ursaki, and E. V. Rusu, Physica B **353**, 111 (2004).
[8]E. Furno, F. Bertazzi, M. Goano, G. Ghione, and E. Bellotti, Solid-State Electron. **52**, 1796 (2008).
[9]B. Gil and A. V. Kavokin, Appl. Phys. Lett. **81**, 748 (2002).